Journal of Hazardous Materials 163 (2009) 315–322

Contents lists available at ScienceDirect

Journal of Hazardous Materials

journal homepage: www.elsevier.com/locate/jhazmat

Effect of quartz sand replacement by agate rejects in triaxial porcelain

Sivaldo L. Correia [a], Gracieli Dienstmann [a], Marilena V. Folgueras [a], Ana M. Segadaes [b,*]

[a] State University of Santa Catarina, Centre of Technology Sciences (UDESC/CCT), 89223-100 Joinville, SC, Brazil
[b] University of Aveiro, Department of Ceramics and Glass Engineering (CICECO), 3810-193 Aveiro, Portugal

ARTICLE INFO

Article history:
Received 6 March 2008
Accepted 24 June 2008
Available online 3 July 2008

Keywords:
Agate
Quartz
Porcelain
Experiments design
Environment
Industrial rejects

ABSTRACT

The ceramics industry, given the high volume of materials processed, stands as one of the largest consumers of natural raw materials but has also the capacity and potential to make significant contributions to solving environmental problems associated with other industries rejects. This work investigates the effects of quartz sand replacement by agate rejects (scrap) in a traditional triaxial porcelain composition. The study was carried out using the design of experiments (DoE) method. Characterization results were used to calculate statistically significant and valid regression equations, relating dried and fired body properties with clay, feldspar and agate scrap contents in the unfired mixture. The regression models were then discussed against X-ray diffraction and scanning electron microscopy results and used simultaneously to delimit the combinations of those three raw materials most adequate to produce a porcelainized stoneware floor tile with specified properties. Thus, an alternative use of an otherwise waste material is proposed, which can be translated into economic benefits and an important and welcome relief on environmental and waste disposal concerns.

1. Introduction

Current increasing industrialization is placing an enormous pressure on the environment through the volume of natural materials consumed, the amount of waste produced and the amount of energy used. The optimization of fabrication processes has contributed to a significant reduction of the amount of waste generated, which can no longer be regarded as having zero cost. Industrial wastes must be disposed of at a suitable landfill site or conditioned and kept in-doors. Both procedures cost money, which is driving the need to find suitable inertization treatments for hazardous wastes and alternative uses for non-hazardous wastes [1–3]. Recycling, not only in the processes of origin, but also in other industrial activities, can help solving important issues related to wastes storage and the preservation of limited natural raw materials supplies. To take full advantage of the available opportunities, wastes must be regarded as possible raw materials and, as such, carefully characterized in order to correctly predict their behaviour during processing and their effects on the final products.

The ceramics industry, given the high volume of materials processed, stands as one of the largest consumers of natural raw materials but has also the capacity and potential to make significant contributions to solving problems associated with wastes [4]. Research results from the past few years have shown that ceramic products can incorporate different types of industrial rejects, including those potentially hazardous, without degradation of properties [5–10], which suggests that the ceramics industry might become the natural end-user of other industries' waste materials. Although clay-based ceramics show a natural forgiveness towards the incorporation of a variety of materials, in any given ceramic industry the type of processing tends to be kept constant, with only enough flexibility to accommodate eventual changes in raw materials. Thus, the use of industrial wastes as alternative raw materials can be considered viable only if the host industrial process remains essentially unchanged and the quality and characteristics of the product are not unduly affected.

Agate is a microcrystalline quartz mineral, a variety of chalcedony, commonly used in the form of semiprecious gemstones, ornamental objects and grinding media. Most agates occur as hollow boulders of eruptive rocks or ancient lavas and show a distinctive banded structure of peculiar shape and colour, which is not disturbed during crystallization. Successive layers lie approximately parallel to the rock surface and can be seen in cross sections, generally used for best aesthetic purposes.

Agate can be found in several Brazilian states but Paraná (PR), Santa Catarina (SC) and Rio Grande do Sul (RS), in southern Brazil, are the major producers of these gemstones. During stone beneficiation, a significant amount of agate scrap is produced, which includes the powder generated in the stone cutting and dry grinding operations.

* Corresponding author. Tel.: +351 234 370 236; fax: +351 234 370 204.
E-mail address: segadaes@ua.pt (A.M. Segadaes).

0304-3894/$ – see front matter © 2008 Elsevier B.V. All rights reserved.
doi:10.1016/j.jhazmat.2008.06.094

Being a non-hazardous industrial sub-product, agate scrap can be included in the large group of industrial wastes that are similar in composition to the natural raw materials used in the ceramic industry and can be not only compatible but also beneficial in the fabrication of ceramics [7,11].

Porcelain and other traditional ceramics are processed from three types of raw materials, namely plastic materials (generally clays), fluxing materials (usually feldspars) and inert materials or fillers (commonly quartz), which explains the label "triaxial" generally used to designate such ceramic systems [12]. Thus, agate scrap might be usable as inert material or filler, replacing the usual quartz sand, but might also have some beneficial effect on the vitrification behaviour and microstructure development of porcelain.

When the processing conditions are kept constant, as is the tendency in the ceramics industry, a number of properties of dried and fired bodies are basically determined by the combination (or mixture) of those three types of raw materials. This is the fundamental assumption in the statistical design of mixture experiments (DoE) used to obtain a mathematical description of any given property [13–15]. The use of this methodology in the fabrication of ceramics enables the prediction, in an expeditious way, of the effects of a change in raw materials, or the proportions thereof, on the various processing steps towards the final product. A detailed description of the procedure can be found elsewhere [16,17], showing how to accommodate restrictions imposed by processing on the raw materials contents (the pseudo-component concept), the need for replications of the experiments to better the confidence in the experimental results and guarantee their reproducibility, and how a regression polynomial is fitted to the experimental values and validated.

In the present work, to investigate the suitability of quartz sand replacement and optimize the agate scrap content, the DoE methodology was used to mathematically model the physical–mechanical properties, as functions of the proportions of clay, feldspar and agate scrap present in the mixture of raw materials, under constant processing conditions. The models so obtained can then be used to select the best combination of those three raw materials to produce, using that processing route, a porcelain ceramic body with specified properties.

2. Experimental procedure

The raw materials used were kaolinitic clay supplied by Mineração Tabatinga (Tijucas do Sul, PR, Brazil), potash feldspar supplied by Colorminas (Criciúma, SC, Brazil) and agate scrap powder supplied by Aduvi Pedras do Brasil (Salto do Jacuí, RS, Brazil). The chemical analysis of the raw materials was carried out by X-ray fluorescence (Philips PW 2400 wavelength dispersive fluorescence spectrometer, with Rh X-ray tube). The major crystalline phases were identified by X-ray diffraction (Philips X'PERT diffractometer with monochromatic Cu $K\alpha_1$ radiation, and the JCPDS X-ray data files) and quantified by rational analysis [18].

A {3,2} centroid simplex-lattice design, augmented with interior points, was used to define the ten mixtures of those raw materials that should be investigated. For each of these powder mixtures, the particle size distribution was determined with a Cilas 1064 L particle size analyzer, after dispersing in de-ionized water containing a few drops of deflocculant.

The processing methodology was kept constant and close to the conventional porcelainized stoneware wall and floor tile industrial practice. Mixtures with the selected compositions were wet ground (residue left in a 325 mesh sieve below 1 wt.%), dried (24 h), moisturized (7.0 ± 0.3 wt.%, dry basis) and granulated, to simulate the customary industrial slip spray-drying step, and uniaxially pressed at 40 MPa (EMIC, 10 ton hydraulic press) to produce test bars (70 mm × 25 mm × 5 mm, 20.0 g of material per test piece). The test pieces were dried (110 ± 5 °C until constant weight) and fired at 1180 °C for 1 h (heating at 5.0 °C/min), followed by natural cooling. For each composition, two independent batches were prepared and processed (replications).

The bulk density of dried (DBD) and fired (FBD) test pieces was calculated geometrically, using the dimensions (1 μm resolution Mitutoyo MDC-25 M digital micrometer) and weight (Denver DE 100A digital analytical scale with a resolution of 1 mg) of the test pieces. The water absorption (WA) was determined using Archimedes' liquid displacement method by immersion in boiling water for 2 h. For each mixture, the final test result was taken as the average of the measurements carried out on five test pieces.

The linear firing shrinkage (LFS) was calculated from the change in length, upon firing, of the test bars (measured with Mitutoyo callipers with a resolution of 0.05 mm).

The modulus of rupture of fired test pieces (MoR) was determined in three-point bending tests (EMIC digital test machine with a 1 mm/min cross-head speed, until rupture). For each mixture, the final test result was taken as the average of the measurements carried out on ten test bars.

The major crystalline phases present on fired samples were identified by X-ray diffraction and their microstructure was studied on fracture surfaces (*in natura* and after HF-etching) by scanning electron microscopy (SEM, Zeiss DSM 940, with an Energy Dispersion X-ray detector).

The results obtained for LFS, MoR, WA, DBD and FDB in the two replications were used to iteratively calculate the coefficients of statistically relevant regression equations (models) and response surfaces, relating those properties with the proportions of the clay, feldspar and agate scrap present in the unfired mixture. The calculations were carried out with Statistica 7.1 (StatSoft Inc., 2005).

3. Results and discussion

3.1. Mixture compositions

The chemical (XRF) and mineralogical (rational analysis) compositions of the kaolinitic clay, potash feldspar and agate scrap are presented in Table 1. The three raw materials define the triaxial composition triangle, shown in Fig. 1.

The chosen processing conditions require that lower bound composition limits are used, and those were 20 wt.% clay, 15 wt.%

Table 1
Chemical (XRF) and mineralogical (rational analysis) compositions of clay, feldspar and agate scrap (wt.%)

Constituents	Clay	Feldspar	Agate scrap
Chemical analysis			
SiO_2	46.25	65.35	98.46
Al_2O_3	35.27	19.11	0.21
Fe_2O_3	2.11	0.04	0.02
TiO_2	1.52	0.01	0.01
CaO	0.06	0.21	0.05
MgO	0.30	0.07	0.02
Na_2O	0.05	3.33	0.09
K_2O	1.15	11.64	0.01
L.O.I.	13.21	0.16	1.13
Mineralogical composition			
Kaolinite	86.00	–	–
Muscovite	4.00	–	–
Gibsite	4.00	–	–
Microcline	–	96.10	–
Quartz	4.00	–	98.00
Other	2.00	3.90	2.00

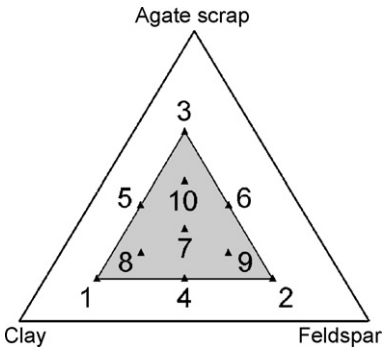

Fig. 1. The raw materials triangle for the triaxial system clay–feldspar–agate, showing the restricted pseudo-components triangle (light grey) and the simplex points (studied compositions).

feldspar and 15 wt.% agate scrap. Thus, a restricted composition triangle of pseudo-components was created (coloured grey, in Fig. 1) on which a {3,2} augmented centroid simplex lattice (ten points) was set. These ten composition points, also shown in Fig. 1, represent the mixtures to be investigated.

3.2. Measured properties and statistical analysis

Table 2 presents the measured values for LFS, MoR, WA, DBD and FDB obtained for the two replications of the ten mixtures. With such data, a regression equation was sought for each property, subjected to a significance level of 5%, and the final results are shown in Table 3. These equations are all referred to the triaxial components clay, feldspar and agate (x_1, x_2 and x_3, respectively) so that mixed raw materials can easily be used (i.e. raw materials which do not lie on the apexes of the composition triangle in Fig. 1).

Table 4 shows the results of the variance analysis of the regressions obtained for LFS, MoR, WA, DBD and FDB (major statistical properties: p value, coefficient of multiple determination R^2, and adjusted coefficient of multiple determination, R^2_A), using the nomenclature commonly found in the literature [14,15]. It can be seen that all models are statistically significant at the required level (p value $\leq$ significance level) and present small variability (high coefficients of multiple determination).

Table 4 also presents the results of lack-of-fit tests, used to check the adequacy of the models. In these tests, the p value exceeds the significance level, meaning that the models do not display lack of fit [14,15]. In all cases, the errors could be considered randomly distributed around a zero mean value (i.e. are uncorrelated), which suggests a common constant variance. On the basis of this analysis, the regression models obtained were accepted to describe the effect of raw materials contents on LFS, MoR, WA, DBD and FDB.

The effect of each raw material on the studied properties can be best visualized in terms of constant contour plots of the properties surfaces, within the pseudo-components triangle.

3.3. Ceramic processing properties: dried body

The particle size distributions in all ten compositions were found to be bimodal, peaking first between 1 and 5 μm (corresponding to clay particles) and then between 10 and 20 μm (corresponding to agate and feldspar particles), all particles being below 40 μm. This suggests high sinterability and optimizes the effect of quartz in the

Table 2
Measured values of LFS, MoR, DBD, FDB and WA obtained for two replications of the ten simplex mixtures

Mixture	LFS (%)	MoR (MPa)	DBD ($g\,cm^{-3}$)	FDB ($g\,cm^{-3}$)	WA (%)
Replication 1					
1	10.03 ± 0.10	41.80 ± 4.82	1.79 ± 0.01	2.16 ± 0.01	6.38 ± 0.21
2	13.62 ± 0.13	54.54 ± 5.52	1.57 ± 0.01	2.33 ± 0.01	0.07 ± 0.02
3	3.01 ± 0.10	12.69 ± 1.36	1.71 ± 0.01	1.75 ± 0.01	15.37 ± 0.26
4	10.14 ± 0.15	57.98 ± 2.77	1.77 ± 0.01	2.31 ± 0.01	0.13 ± 0.03
5	6.46 ± 0.16	25.70 ± 2.47	1.76 ± 0.01	2.00 ± 0.01	9.80 ± 0.36
6	7.67 ± 0.11	27.01 ± 2.59	1.69 ± 0.01	2.18 ± 0.01	3.68 ± 0.14
7	6.23 ± 0.17	31.86 ± 4.12	1.79 ± 0.01	2.14 ± 0.01	6.12 ± 0.24
8	6.32 ± 0.11	29.95 ± 3.38	1.84 ± 0.01	2.15 ± 0.01	5.27 ± 0.31
9	9.78 ± 0.15	47.04 ± 3.53	1.75 ± 0.01	2.30 ± 0.01	0.15 ± 0.02
10	5.12 ± 0.13	19.58 ± 1.90	1.76 ± 0.01	1.96 ± 0.01	10.41 ± 0.42
Replication 2					
1	[a]	[a]	1.82 ± 0.01	[a]	5.84 ± 0.26
2	[a]	[a]	1.63 ± 0.01	2.30 ± 0.01	[a]
3	2.29 ± 0.07	14.02 ± 1.02	[a]	1.78 ± 0.01	14.49 ± 0.31
4	8.74 ± 0.09	[a]	1.78 ± 0.01	[a]	[a]
5	5.95 ± 0.12	26.35 ± 1.32	1.77 ± 0.01	1.97 ± 0.01	9.03 ± 0.16
6	[a]	32.71 ± 2.52	1.73 ± 0.01	2.15 ± 0.01	3.97 ± 0.11
7	[a]	26.93 ± 2.51	1.76 ± 0.01	[a]	4.63 ± 0.17
8	7.67 ± 0.14	29.95 ± 3.38	1.81 ± 0.01	2.18 ± 0.01	[a]
9	11.41 ± 0.17	51.48 ± 3.47	1.71 ± 0.01	2.34 ± 0.01	[a]
10	4.66 ± 0.12	21.32 ± 1.73	1.74 ± 0.01	1.92 ± 0.01	11.26 ± 0.23

[a] Some values could not be measured. Calculated averages refer to available values.

Table 3
Regression equations obtained for LFS, MoR, DBD, FDB and WA (x_1, x_2, and x_3 are the clay, feldspar, and agate fractions, respectively)

Regression model	Property equation
Quadratic	$LFS = 16.16x_1 + 28.21x_2 - 2.06x_3 - 43.49x_1x_2 - 7.10x_1x_3 - 12.33x_2x_3$
Special cubic	$MoR = -8.56x_1 + 11.34x_2 - 39.45x_3 + 431.43x_1x_2 + 249.86x_1x_3 + 300.34x_2x_3 - 1820.89x_1x_2x_3$
Quadratic	$DBD = 1.73x_1 + 1.14x_2 + 1.56x_3 + 1.32x_1x_2 + 0.28x_1x_3 + 1.02x_2x_3$
Quadratic	$FBD = 2.13x_1 + 2.15x_2 + 2.21x_3 + 1.12x_1x_2 + 0.08x_1x_3 + 1.83x_2x_3$
Special cubic	$WA = 19.94x_1 + 19.09x_2 + 43.07x_3 - 117.52x_1x_2 - 81.42x_1x_3 - 144.30x_2x_3 + 440.30x_1x_2x_3$

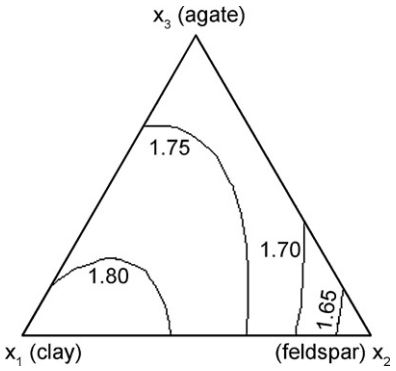

Fig. 2. Predicted dried body bulk density (DBD) constant contour plot (g cm^{-3}) as a function of composition.

final sintered body [19,20]. Also, it is a guarantee that the green body density will not change significantly with the mixture composition.

Fig. 2 shows the constant contour plot for the dry bulk density, as obtained from the corresponding regression equation presented in. The highest dry bulk density values (DBD $\geq$ 1.80 g cm^{-3}) are reached in the composition area corresponding to high contents of plastic material (clay contents of 50–70 wt.%, feldspar and agate below 30 wt.%). This can probably be explained by a particle packing effect, since both agate scrap and feldspar contain larger particles [12]. Nevertheless, the DBD has the expected narrow variation range (1.73 ± 0.075 g cm^{-3}, Table 2) and should not have a significant effect on the fired body bulk density (FBD).

3.4. Ceramic processing properties: fired body

The effects of raw materials on fired body bulk density and water absorption can be seen on the constant contour plots in Fig. 3, obtained from the corresponding regression equations in Table 3. Fig. 3a shows no similarity with the DBD contour plot, confirming that the observed changes in FBD are not caused by differences in DBD. Fig. 3a also shows that FBD is nearly independent of the clay content and the highest FBD occurs for agate/feldspar weight ratios below 0.25, i.e. under the conditions used in this work, high agate contents adversely affect FBD. As expected, Fig. 3b shows the inverse trend, that is, increasing agate contents favour an increase in WA, while increasing feldspar content contributes to lower WA. Fig. 3b also shows that there is a comfortable composition range of low-to-medium agate/feldspar weight ratios (below 0.45) to obtain low WA (WA $\leq$ 2.0 wt.%).

Fig. 4 shows the effects of raw materials on the linear firing shrinkage and bending strength (MoR), as constant contour plots obtained from the corresponding regression equations in Table 3. It can be seen, from Fig. 4a and the coefficients in the LFS equation in Table 3, that feldspar (x_2) has the strongest effect on LFS, followed by the clay (x_1). Fig. 4a also shows that the compositions with the best (lowest) WA values (Fig. 3b) also present the highest firing shrinkage. Nevertheless, low firing shrinkage values (e.g.

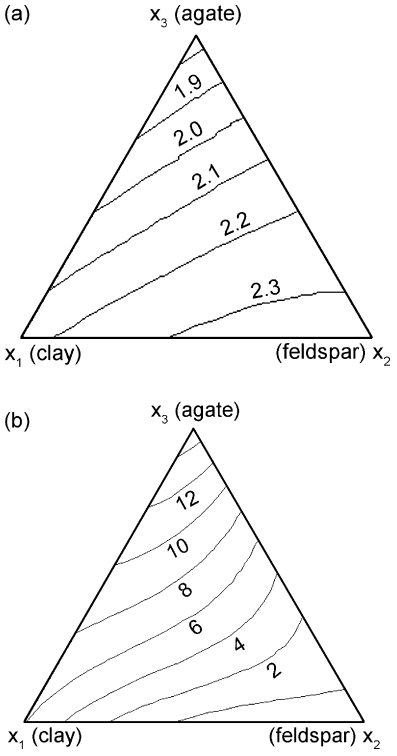

Fig. 3. Predicted fired body properties constant contour plots as a function of composition: (a) bulk density (FBD, g cm^{-3}), and (b) water absorption (WA, %).

below 8.0%) can be reached within a broad composition area, for agate contents above 50 wt.% and feldspar contents below 30 wt.%.

The effects of raw materials on the bending strength of fired ceramic bodies (MoR), shown in Fig. 4b, are similar to those

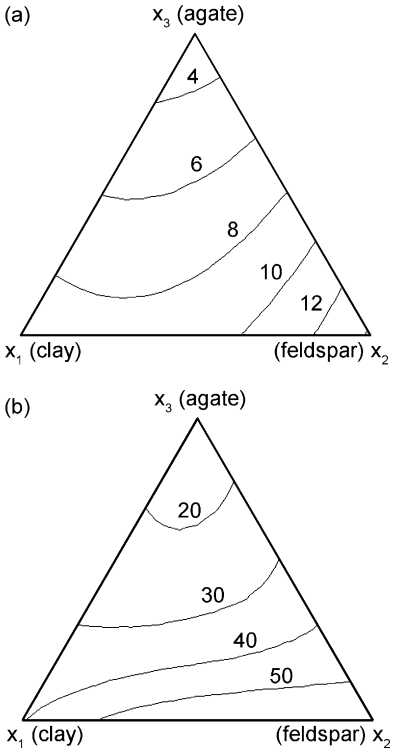

Fig. 4. Predicted fired body properties constant contour plots as a function of composition: (a) firing shrinkage (LFS, %), and (b) flexural strength (MoR, MPa).

Table 4
Major statistical properties, relevant for variance analysis and lack-of-fit tests

Property	Regression model	Variance analysis results			Lack-of-fit results
		p value	R^2	R^2_A	p value
LFS	Quadratic	0.0476	0.9460	0.9189	0.2970
MoR	Special cubic	0.0377	0.9504	0.99207	0.1391
DBD	Quadratic	0.0006	0.9149	0.8821	0.6601
FBD	Quadratic	0.0033	0.9796	0.9703	0.0744
WA	Special cubic	0.0292	0.9804	0.9675	0.0829

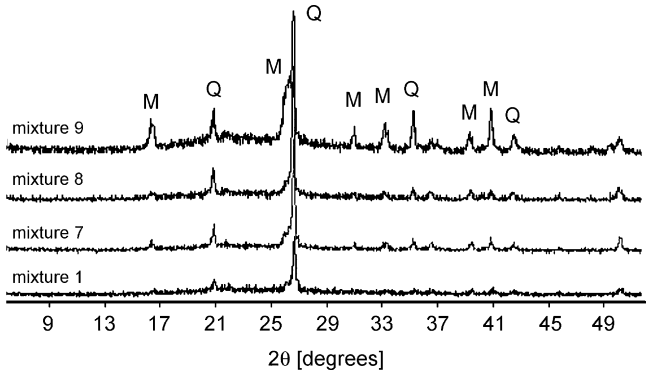

Fig. 5. X-ray diffraction patterns of fired compositions 1, 7, 8 and 9 (refer to Fig. 1 for composition location): Q, quartz; M, mullite.

observed for the fired bulk density (FBD), shown in Fig. 3a, confirming the strong influence of FBD on MoR [21,22]. Figs. 3a and 4b show that the highest (MoR $\geq$ 50 MPa) and the highest FBD were found to occur in same composition range, for agate/feldspar weight ratios below 0.25.

3.5. Microstructure and mechanical behaviour

Quartz and mullite were the major crystalline phases identified by XRD in all fired samples. As an illustration, Fig. 5 shows the X-ray diffraction patterns of compositions 1, 7, 8 and 9 (see Fig. 1 for composition location). Fig. 6 shows the HF-etched fracture surfaces of these samples, as observed by SEM. In these samples, free quartz grains, that remained undissolved in the final microstructure, along with well-interlocked secondary mullite needles, can clearly be seen. These observations agree with the three main theories proposing explanations for the mechanical properties of porcelain [12], which consider that the crystalline phases present, dispersed in the vitreous phase, are the ruling factor influencing the mechanical properties.

Fig. 7 illustrates the differences in pore morphology, as seen on fracture surfaces by SEM, and shows that the raw materials also affect closed pore characteristics and the microstructure (see Fig. 1 for composition location). Upon firing, composition 1 (Fig. 7a) mostly contains isolated and irregular elongated pores, in the 1–20 μm diameter range. Such pore morphology (i.e. irregular and elongated pores) can be due to a higher glass viscosity caused by the low feldspar content, despite the high kaolinitic clay content [6]. Fig. 7a also shows that the fracture surface follows

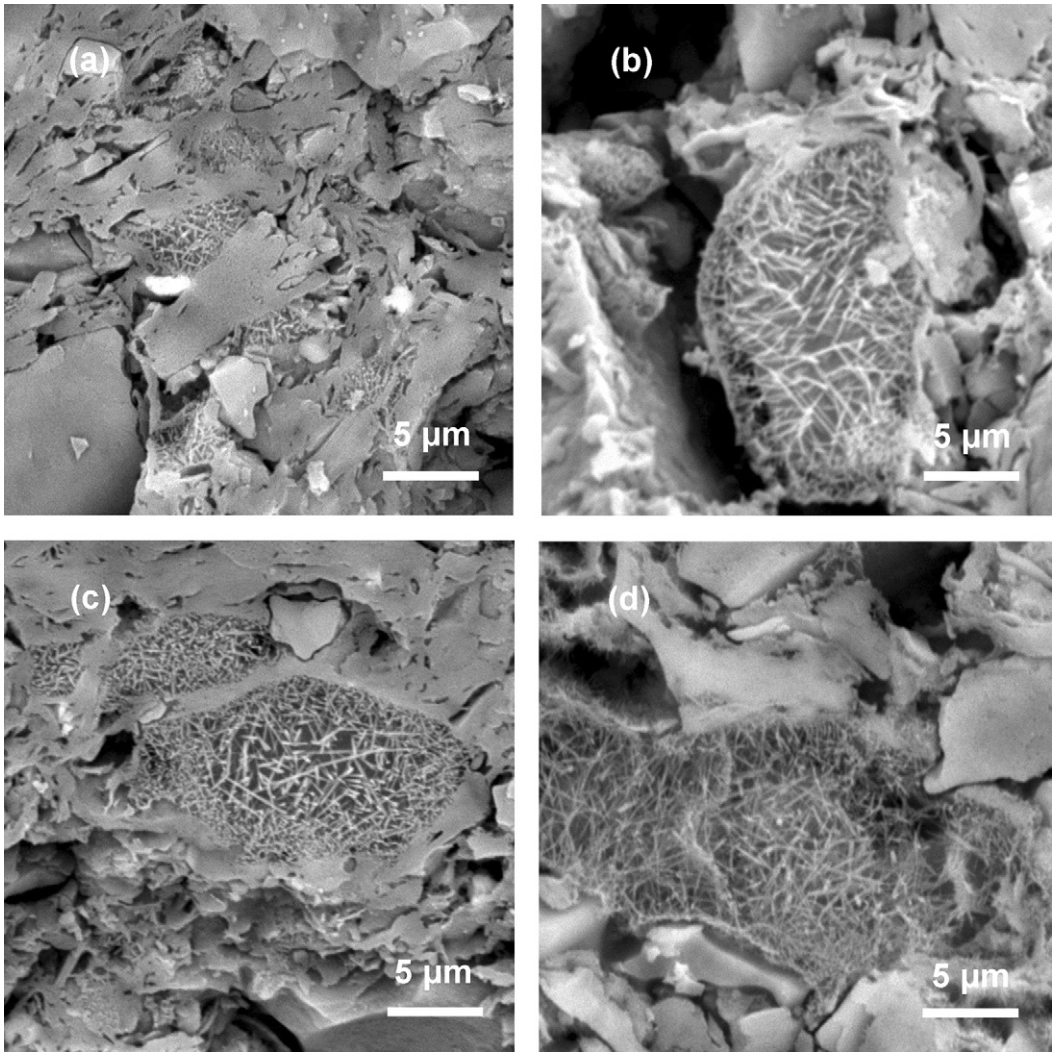

Fig. 6. SEM photographs of HF-etched fracture surfaces of fired samples, showing secondary mullite needles and residual quartz grains in compositions: (a) 1, (b) 7, (c) 8, and (d) 9.

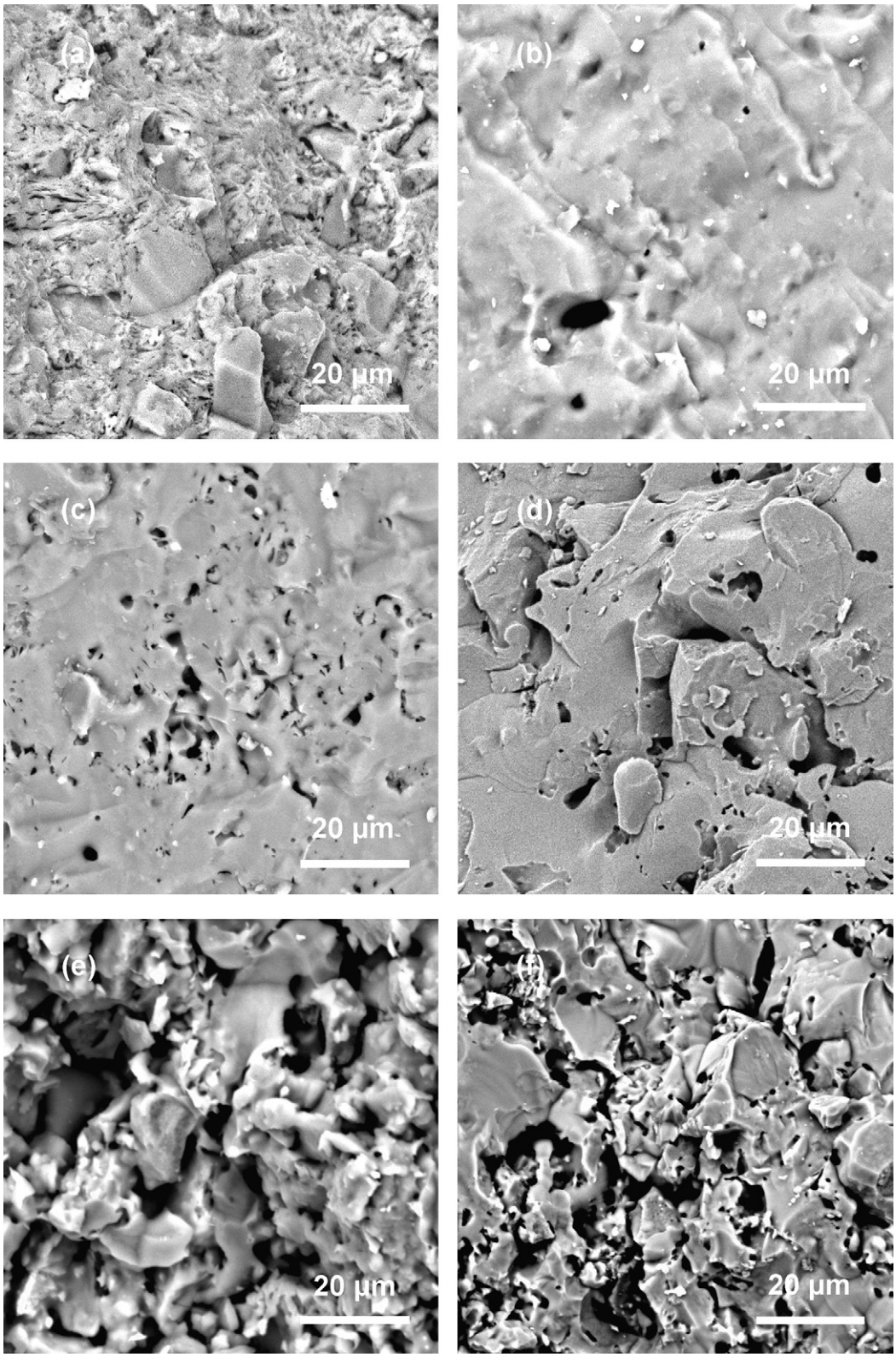

Fig. 7. SEM photographs of fracture surfaces (*in natura*) of fired samples, showing the pore characteristics in compositions: (a) 1; (b) 2; (c) 4; (d) 9; (e) 3; (f) 5.

cracks around quartz grains, linking isolated pores. On the contrary, fired compositions 2, 4 and 9 (Fig. 7b–d) are characterized by isolated, spherical, small pores (1–15 μm). In comparison, compositions 3 and 5 (Fig. 7e and f) are clearly not well sintered, as they are characterized by a large amount of profusely interconnected pores, irregular in shape and in the size range of 10–40 μm (composition 3, Fig. 7e) and 5–20 μm (composition 5, Fig. 7f).

It is generally accepted that bending strength in ceramics decreases exponentially with increasing porosity, very much dependent on the amount of liquid phase present at the firing

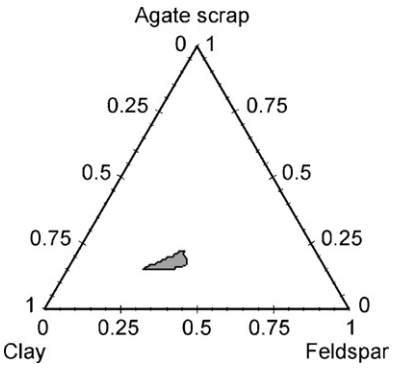

Fig. 8. Intersection of the MoR, FBD, DBD, LFS and WA surfaces (feasible region, shaded) showing the composition range suitable for porcelainized floor tiles production (LFS ≤ 9.0%, MoR ≥ 40 MPa, DBD ≥ 1.80 g cm^{-3}, FBD ≥ 2.20 g cm^{-3} and 0.5% ≤ WA ≤ 3.0%).

temperature, and that, the denser the fired bodies, the higher the bending strength [12,19,23]. The influence of the microstructure on the bending strength (refer to Table 2 for physical–mechanical properties) is evident in some compositions, namely 3 and 5 (Fig. 7e and f). These samples show a very porous microstructure (high water absorption), which is clearly detrimental for the mechanical properties.

3.6. Applicability, subjected to restrictions in product specification

Assuming that the raw materials and processing method studied in this work were to be used in the production of porcelainized floor tiles, hence in the AI (extruded) or BI (pressed) groups specified by the European standard EN 87 [24] or the Brazilian standard ABNT 13818 [25], a set of constraints can be placed on the characteristics of the final product, namely on the values of MoR, FDB and WA:

$$\text{MoR} \geq 40\,\text{MPa}, \quad \text{FDB} \geq 2.20\,\text{g cm}^{-3} \text{ and } 0.5\% \leq \text{WA} \leq 3.0\% \qquad (1)$$

Fabrication imposes extra constraints, namely on the DBD and the LFS (handling of unfired products, raw materials procurement, die sizes):

$$\text{DBD} \geq 1.80\,\text{g cm}^{-3} \text{ and } \text{LFS} \leq 9.0\% \qquad (2)$$

The selection of an adequate mixture composition range (feasible region) to satisfy all constraints translates into finding a graphical solution (i.e. intersection) of equations in Table 3 (or the constant contour plots represented in Figs. 2–4) combined with the inequalities (1) and (2).

Fig. 8 shows the composition area (feasible region, shaded) suitable for the production of porcelain stoneware floor tiles with the desired properties, i.e. within which LFS ≤ 9.0%, MoR ≥ 40 MPa, DBD ≥ 1.80 g cm^{-3}, FBD ≥ 2.20 g cm^{-3} and 0.5% ≤ WA ≤ 3.0%.

For the particular raw materials and processing conditions used in this work, the results obtained (Fig. 8) show that there is a rather forgiving composition range of clay (43–60 wt.%), feldspar (25–37 wt.%) and agate scrap (15–22 wt.%) contents capable of meeting the imposed requirements. Those mixtures present close values of linear firing shrinkage, bending strength, dried and fired bulk density and water absorption, all within the specified properties range of values.

4. Conclusions

The results obtained in this work show that a non-beneficiated reject material obtained from the agate extraction and beneficiation industry (agate scrap) can be used to replace the traditional quartz sand in the porcelainized stoneware floor tile industrial fabrication with no major sacrifice to the properties of the final product or the fabrication process. Such an alternative use of an otherwise useless material can be translated into economic benefits and an important and welcome relief on environmental and waste disposal concerns.

The design of mixture experiments and the use of response surface methodologies enabled the calculation of regression models relating the dried and fired ceramic bodies properties, after the same processing, with the raw materials original contents. Those models were then used to find the best combination of the particular raw materials to produce a ceramic body with specified properties.

The use of intersecting surfaces showed that, for the particular raw materials and fabrication process under consideration, there is a rather forgiving composition range of kaolinitic clay (43–60 wt.%), potash feldspar (25–37 wt.%) and agate scrap (15–22 wt.%) within which it is possible to simultaneously specify the values of various technological properties, not only of the fired products but also of the intermediate materials at important stages of the processing.

Acknowledgements

The authors appreciate the financial support received from UDESC-Joinville (project DAPE 04/2005, S. L. Correia) and the Brazilian Research Agency CNPq (G. Dienstmann, grant), and are thankful to Aduvi Pedras do Brasil (Salto do Jacuí, RS), Colorminas (Criciúma, SC) and Mineração Tabatinga (Tijucas do Sul, PR) for providing the raw materials used throughout the work.

References

[1] J. Sorvari, By-products in earth construction—environmental assessments, J. Environ. Eng. 129 (2003) 899–909 (Special issue: Recycling of Waste Materials in Construction).
[2] M.C. Shinzato, R. Hypolito, Solid waste from aluminum recycling process: characterization and reuse of its economically valuable constituents, Waste Manage. 25 (2005) 37–46.
[3] F. Andreola, L. Barbieri, A. Corradi, I. Lancellotti, Cathode ray tube glass recycling: an example of clean technology, Waste Manage. Res. 23 (2005) 1–8.
[4] W.E. Lee, A.R. Boccaccini, J.A. Labrincha, C. Leonelli, C.H. Drumond-III, C.R. Cheeseman, Green engineering—ceramic technology and sustainable development, Am. Ceram. Soc. Bull. 86 (2007) 18–25.
[5] L.P.F. Souza, H.S. Mansur, Production and characterization of ceramic pieces obtained by slip casting using powder wastes, J. Mater. Proc. Technol. 145 (2004) 14–20.
[6] A. Tucci, L. Esposito, E. Rastelli, C. Palmonari, E. Rambaldi, Use of soda-lime scrap-glass as a fluxing agent in a porcelain stoneware tile mix, J. Eur. Ceram. Soc. 24 (2004) 83–92.
[7] A.M. Segadães, M.A. Carvalho, W. Acchar, Using marble and granite rejects to enhance the processing of clay products, Appl. Clay Sci. 30 (2005) 42–52.
[8] M. Erol, S. Küçükbayrak, A. Ersoy-Meriçboyu, Comparison of the properties of glass, glass–ceramic and ceramic materials produced from coal fly ash, J. Hazard. Mater. 153 (2008) 418–425.
[9] A.M. Segadães, Use of phase diagrams to guide ceramic production from wastes, Adv. Appl. Ceram. 105 (2006) 46–54.
[10] F. Raupp-Pereira, M.J. Ribeiro, A.M. Segadães, J.A. Labrincha, Extrusion and property characterisation of waste-based ceramic formulations, J. Eur. Ceram. Soc. 27 (2007) 2333–2340.
[11] W. Acchar, E.G. Ramalho, Y.A. Fonseca, D. Hotza, A.M. Segadães, Using granite rejects to aid densification and improve mechanical properties of alumina bodies, J. Mater. Sci. 40 (2005) 3905–3909.
[12] W.M. Carty, U. Senapati, Porcelain—raw materials, processing, phase evolution and mechanical behavior, J. Am. Ceram. Soc. 81 (1998) 3–20.
[13] L.Y. Chan, Optimal designs for experiments with mixtures: a survey, Commun. Stat. A Theor. 29 (2000) 2281–2312.
[14] R.H. Myers, D.C. Montgomery, Response Surface Methodology: Process and Product Optimization Using Designed Experiments, Wiley, New York, 2002.
[15] J.A. Cornell, Experiments with Mixtures: Designs, Models and the Analysis of Mixture Data, third ed., Wiley, New York, 2002.
[16] S.L. Correia, K.A.S. Curto, D. Hotza, A.M. Segadães, Using statistical techniques to model the flexural strength of dried triaxial ceramic bodies, J. Eur. Ceram. Soc. 24 (2004) 2813–2818.
[17] S.L. Correia, D. Hotza, A.M. Segadães, Application of mathematical and statistical strategies to optimize ceramic bodies: effects of raw materials on the technological properties, CFI – Ceram. Forum Int. 82 (2005) E39–E43.

[18] C. Coelho, N. Roqueiro, D. Hotza, Rational mineralogical analysis of ceramics, Mater. Lett. 52 (2002) 394–398.
[19] O.I. Ece, Z.E. Nakagawa, Bending strength of porcelains, Ceram. Int. 28 (2002) 131–140.
[20] G. Stathis, A. Ekonomakou, C.J. Stournaras, C. Ftikos, Effect of firing conditions, filler grain size and quartz content on bending strength and physical properties of sanitaryware porcelain, J. Eur. Ceram. Soc. 24 (2004) 2357–2366.
[21] W.D. Callister, Materials Science and Engineering, Wiley, New York, 2000.
[22] S.R. Bragança, C.P. Bergmann, Traditional and glass powder porcelain: technical and microstructure analysis, J. Eur. Ceram. Soc. 24 (2004) 2383–2388.
[23] Y. Kobayashi, O. Ohira, E. Kato, Effect of firing temperature on bending strength of porcelains for tableware, J. Am. Ceram. Soc. 75 (1992) 1801–1806.
[24] European standard EN 87: ceramic floor and wall tiles—definitions, classification, characteristics and marking, 1992.
[25] ABNT-Brazilian Association for Technical Standards, NBR 13818, Annex C: Ceramic Tiles—Specifications and Test Methods, 1997, pp. 14–16 (in Portuguese).